Discrete Fracture Network Simulation: Application of Tectonic Simulation and Conditional Global Optimization Technique*

Nima Gholizadeh Doonechaly[1] and Sheik Rahman[1]

Search and Discovery Article #40861 (2012)
Posted January 9, 2012

*Adapted from extended abstract prepared in conjunction with oral presentation at AAPG International Conference and Exhibition, Milan, Italy, October 23-26, 2011

[1]University of New South Wales, Sydney, NSW, Australia (z3277971@student.unsw.edu.au)

Abstract

Modeling of naturally fractured reservoirs is associated with the uncertainties due to the lack of sufficient field data. Two major approaches exist to simulate naturally fractured reservoirs, namely tectonic and statistical simulations. Tectonic simulation is a powerful tool to estimate the probability of the presence of fracture based on the deformation history of the basin. Also there exists a wide variety of statistical approaches to model naturally fractured reservoirs. In this study a combination of tectonic and statistical modeling technique is utilized to get more accurate results. Finite element method is used to model folding/unfolding of tectonic events to construct a 3D map of fracture probability in the reservoir layer. Then an object based conditional global optimization technique is used to integrate results of the tectonic simulation and all other field data, such as seismic attributes, core descriptions, borehole images, well logs etc. to simulate the discrete fracture network. The proposed hybrid model improves the results over existing modeling techniques such as, stochastic simulation due to utilizing continuous data in both horizontal and vertical directions. The methodology is presented through a case study of Palm Valley gas Field in Australia. The results show that the model is able to simulate discrete fracture network of petroleum reservoir with great accuracy while hard data is not available.

Introduction

Comprehensive discrete fracture network (DFN) models provide an understanding of the reservoir make up and help select the best locations for production wells, study the response of natural fractures under induced stimulation pressure and develop optimum

production methods to maximize recovery (Nelson, 1982). There exist two distinct approaches to discrete fracture network modeling. They include tectonic and statistical approaches. Tectonic theories have been used extensively in the past to generate discrete fracture networks (Price, 1966; Reddy and Wickham, 1983; Wickham and Reddy, 1983; Cosgrove, 1999; Jager et. al., 2008). This involves estimation of stress distribution during folding and/or unfolding of a layer due to tectonic events. Folding and unfolding have been modeled numerically by fluid mechanics theories with the assumption that the rock is treated as nearly incompressible fluid (Odriscoll, 1962; Ramberg, 1963; Schmalholz, 2008). Schmalholz (2008) showed that 3D folds can be accurately restored to their original shape in a single extension event (reverse model) in a reversible process. This reversibility is the key point in reconstruction of folded layers in a consecutive unfolding and folding event. During the folding event, the stress distribution can be calculated for all parts of the layer based on the deformation (strain rate). The stress invariants obtained from calculated stress tensor are used to estimate the probability of occurrence of fractures. Most of the developed tectonic models are based on the assumption that rock behaves as a Newtonian Fluid. It was found that the rock viscosity changes due to the deformation and this change can be simulated by different models such as Oswald de Waele's (Parish, 1976). Also in the tectonic models, none of the real field data such as seismic, logs, and cores are used in the fracture network simulation process. The parameters, that can be used, are the initial shape of the formation layer and its material properties (viscosity, density, etc.). Simplification of such a complex problem makes the numerical modeling of tectonic events unreliable. The above problem has been adequately addressed in geostatistical modeling. Statistical approaches that are used to model discrete fracture networks are mainly based on the spatial distribution of parameters and their inter-relationship (Jensen et. al., 2010). For this purpose, a wide variety of techniques are used to characterize different properties of a naturally fractured reservoir and then geostatistical techniques are used to model discrete fractures (Gringarten, 1998). One example the use of stochastic simulation in petroleum reservoir is geological modeling (Bahar et. al., 2003; Bogatkov and Tayfun, 2008; Rafiee, 2008). As opposed to deterministic interpolation, the stochastic simulation provides the opportunity to run local uncertainty analysis. It employs Monte Carlo sampling in a selective and random scheme to generate multiple equiprobable realizations based on specific statistical properties. Many authors have also used sequential Gaussian stochastic simulation method as a very powerful stochastic simulation technique (Sahimi, 1995; Tamagawa et. al., 2002; Tran et. al. 2006). However stochastic simulation techniques, represent an integrated approach, there are uncertainties associated with the fracture distributions far from the wellbore since the field data are mostly available near well locations. Also results of the stochastic simulations are hard to validate. To overcome these limitations some complex methodologies were developed such as neural networks. They can integrate wellbore data from different scales. However they can not simulate the fractures in an objective manner and they can only provide a fracture density map in different parts of a reservoir. In the present study a hybrid technique is used to model the discrete fracture network in a naturally fractured reservoir (Palm Valley Gas Field, Australia). This hybrid methodology consists of tectonic simulation and object based conditional global optimization. In an object based modeling fractures are generated as discrete objects with their specific properties such as dip, azimuth and radius. There is no need to make any assumption for the parts of the reservoir which field data is not available. In the first part of this study Finite

Element Method (FEM) is used to reconstruct a folded layer by unfolding and folding (reverse and forward model) in a single tectonic event. Also a non-linear flow model is used to consider the effect of deformation on rock viscosity. After reconstructing the original shape of the layer, stress tensor values as well as the stress invariants are calculated for each node based on the deformation history of the model. Mohr-Colomb fracture criterion, which relates the critical strength of the material to its stress state, is used to determine whether the obtained stress exceeds strength (shear) of rock. If the obtained stress tensor satisfies failure criterion, stress invariants are used to calculate the rate of formation of fractures for each node. Rate of formation of fractures is used as one of the most important input parameters for the next step which is the global optimization. Then based on the tectonic simulation results, an initial guess for discrete fracture network is generated in a random realization scheme. For this purpose, the rate of formation of fracture is defined for each part of the reservoir and the obtained values are calibrated based on the fracture density map obtained based on the field data. Then the fracture network is randomly generated based on the current calibrated fracture density map. After that, the objective function is defined based on the difference between the generated fracture network and the target obtained based on the real fracture properties obtained from the field data. After the objective function is defined, global optimization technique is used to modify the realization in an iterative scheme to minimize the objective function. When the objective function is minimized, the generated fracture network is the proper representation of the reservoir by using this technique.

Methodology

In the first part of this study a folded layer is extended (reverse model) and then compressed (forward model) to reconstruct the geological folded structure (Kaus and Podladchikov, 2001; Kocher and Mancktelow, 2005). An efficient numerical algorithm using Finite Element Method (FEM) is used to model the reverse and forward folding during sufficient number of time steps. For this purpose mixed penalty finite element formulation is used to model quasi-steady state incompressible viscous flow based on the Navier Stokes flow equation (Cuvelier et. al., 1986; Haupt, 2002). Mixed penalty formulations are based on decomposing stress tensor into its deviatoric and hydrostatic components and can be expressed as:

$$\sigma = s - pm \qquad (1)$$

Where s is the deviatoric stress, p is the pressure (mean sum of normal stresses is considered) and m is expressed as:

$$m^T = [1\ 1\ 1\ 0\ 0\ 0]$$

Also constrained equation which relates the divergence of displacement to the pressure is used to make a link between the stress and strain rate tensor as:

$$\nabla^T . u + \frac{p}{K} = 0 \qquad (2)$$

Where, K is the bulk modulus of the rock. Also the equilibrium of the material dictates the following equation:

$$\nabla\sigma + b = 0 \qquad (3)$$

Combining Eq. (1) and Eq. (3) we have:

$$\nabla\sigma - \nabla p + b = 0 \qquad (4)$$

Equations (2) and (3) are discretised using relevant shape functions. It is important to note that only certain combinations of pressure and velocity shape function interpolations can be used to reach the convergence conditions (Pastor et. al., 1997). In this study the Q2-P1 element with 27 velocity nodes and 4 discontinuous degrees of freedom for pressure are used for the discretization purpose. Pressure nodes are on the corners of a tetrahedral which is located inside the brick element containing the velocity nodes. This is the simplest 3D element which is second-order accurate and satisfies the babuska-brezzi stability condition to avoid the pressure solution to be locked in the unwanted loop (Fortin, 1981).

For numerical modeling purpose, the folded layer is embedded between two heavier layers with lower viscosity to simulate natural condition. To eliminate the effect of surrounding layers on the folding process, the thickness of the layers above and below the reservoir is calculated as follow (Johnson 1970):

$$H = 2\frac{L_D}{\pi} \qquad (5)$$

Where, L_D is the wavelength and H is the thickness of the matrix layer.

In the reverse model, the extension is continued until the folded layer reaches the initial amplitude as (Biot, 1961):

$$\frac{A_0}{h} = 0.1 \qquad (6)$$

Where, A_0 is the initial amplitude and h is the thickness of the layer.
Predetermined velocities (6.31×10^{-9} m/s) are applied on the sides of the model along y direction as boundary condition. The time increment (1000 years in this study) in each step is chosen such that the boundary strain rate remains constant (0.02 percent per thousand years) during the tectonic simulation to satisfy the plate convergence rate of 2 cm/yr which is calculated as (Moore and Karig 1976):

$$\Delta t = L_i \frac{(1-e^{-0.02})}{2u} \qquad (7)$$

Where L_i is the wavelength of the layer and u is the boundary velocity.
After discretization one can obtain the following system of equations:

$$\begin{bmatrix} K & Q \\ Q^T & -\frac{V}{\gamma} \end{bmatrix} \begin{bmatrix} u \\ p \end{bmatrix} = \begin{bmatrix} f \\ g \end{bmatrix} \qquad (8)$$

In which we have:

$$K = \int B^T D B \, d\Omega \qquad (9)$$

$$Q = -\int B^T m \, N_p \, d\Omega \qquad (10)$$

$$V = \int N_p^T N_p \, d\Omega \qquad (11)$$

$$f = \int N_u^T \rho g \, d\Omega + \int N_u^T \bar{t} \, d\Gamma \qquad (12)$$

$$g = -\frac{V}{\gamma} P_n \tag{13}$$

$$D = \mu \begin{bmatrix} 2 & 0 & 0 & 0 & 0 & 0 \\ 0 & 2 & 0 & 0 & 0 & 0 \\ 0 & 0 & 2 & 0 & 0 & 0 \\ 0 & 0 & 0 & 1 & 0 & 0 \\ 0 & 0 & 0 & 0 & 1 & 0 \\ 0 & 0 & 0 & 0 & 0 & 1 \end{bmatrix} \tag{14}$$

Where, B is the discrete operator relating deviatoric strains to nodal displacements (Zienkiewicz and Nithiarasu, 2000), N_u and N_p are velocity and pressure shape functions respectively, μ is the viscosity of the material and γ is the penalty parameter that is used as an estimation of the bulk modulus of the rock. Proper selection of the penalty parameter results in a divergence of 10^{-16} for the velocity unknowns in the iterative solution procedure. Normally penalty number is chosen according to (Hughes, 1987; Bathe, 1996; Zienkiewicz and Nithiarasu, 2000) as:

$$\gamma = (10^7 - 10^8)\,\mu \tag{15}$$

Discontinuous pressure shape functions allow the separation of the pressure at the element level and the solution of the linear system of Eq. (8) is found in the following consecutive steps:

$$g = -\frac{V}{\gamma} Pn \tag{16}$$

$$\left(K + Q^T \frac{V}{\gamma} Q\right) u = f + Q\,\gamma V^{-1} g \tag{17}$$

$$P_{n+1} = (\gamma Q^T V^{-1} u) - (\gamma V^{-1} g) \tag{18}$$

Linear system of unknown parameters (Eq. (8)) is solved using Uzawa type iterative algorithm. First an initial guess is used as the pressure value for all relevant pressure nodes. Then in the next step the "g" matrix is calculated as shown in Eq. (16). Following that, Eq. (17) is solved for velocity unknowns. Finally, new pressure values are calculated for each pressure node based on Eq. (18). Iteration is repeated until the divergence of the velocity reduces to a desired value (10^{-16} m/sec in this study).

After the convergence of the velocity solution is reached, the power law model is used to adjust the viscosity value for each node. For this purpose Oswald - de Waele model as shown in equation (19) is used (Zienkiewicz and Nithiarasu, 2000).

$$\mu = \mu_0 \dot{\varepsilon}^{(m-1)} \qquad (19)$$

Where, μ_0 is the initial viscosity value and ε is the second invariant of the strain rate tensor and m is the flow behavior index. For most of the non-Newtonian fluids, m is smaller than 1 and usually it varies from 0.125 to 0.25 for geological studies. In this study m is taken as to 0.25. Then Uzawa iteration as discussed above is repeated with the new values of viscosities until the divergence of the viscosity reaches 10^{10}. Finally the resulted velocity solution is used to move each node to its new location by multiplying velocity by the time increment in each step. In each time step during unfolding and folding, strain rate tensor is calculated as:

$$\varepsilon = B \cdot u \qquad (20)$$

Where, ε is the strain rate tensor for each node, u is the nodal velocity.

Then stress tensor can be obtained as:

$$\begin{bmatrix}\sigma_{xx}\\ \sigma_{yy}\\ \sigma_{zz}\\ \sigma_{xy}\\ \sigma_{yz}\\ \sigma_{xz}\end{bmatrix} = -p\begin{bmatrix}1\\ 1\\ 1\\ 0\\ 0\\ 0\end{bmatrix} + \frac{1}{3}\mu\begin{bmatrix}4 & -2 & -2 & 0 & 0 & 0\\ -2 & 4 & -2 & 0 & 0 & 0\\ -2 & -2 & 4 & 0 & 0 & 0\\ 0 & 0 & 0 & 3 & 0 & 0\\ 0 & 0 & 0 & 0 & 3 & 0\\ 0 & 0 & 0 & 0 & 0 & 3\end{bmatrix} \times \begin{bmatrix}\varepsilon_{xx}\\ \varepsilon_{yy}\\ \varepsilon_{zz}\\ \varepsilon_{xy}\\ \varepsilon_{yz}\\ \varepsilon_{xz}\end{bmatrix} \qquad (21)$$

Where, σ is the deviatoric stress and p is the pressure which is calculated as:

$$p = \frac{\sigma_{xx} + \sigma_{yy} + \sigma_{zz}}{3}$$

Stress tensors are updated after each time step until the original folded layer is reconstructed. Then stress values at each node are used in the next step as one of the most important input parameters in stochastic simulation. There are also analytical solutions for stress values in 3D single layer folds (Fletcher, 1991), however, such analytical solutions are for small amplitude/limb folds and cannot be used for big scale problems (Schmalholz, 2008). In the forward model, in each time step, the resultant stress tensor value in each node is checked with the Mohr-Colomb fracture criteria to determine whether fracture occurs or not. If the rock passed the failure criterion, the rate of formation of fractures is calculated based on the generalization of the equilibrium thermodynamic as (see Wickham et al. 1982 for the complete derivation):

$$\gamma_f \frac{dA}{dt} = \frac{2}{3\mu}(I_1^2 - 3I_2) - \frac{8}{\mu} K_0 I_1 \qquad (22)$$

Where, I_1 and I_2 are the first and second stress invariants, γ_f is the surface tension energy and K_0 is the material constant. In the above equation, if the $\frac{dA}{dt}$ is less than zero, no fracture exists and greater than zero, probability of fracture exists.

Conditional Global Optimization

After the rate of growth of fractures is identified by using the tectonic simulation, an initial guess of the fracture network is generated in a random scheme. For this purpose, the results obtained from tectonic simulation are calibrated based on the fracture density values given based on the field data. Then a 3D map of the fracture density is generated according to the fracture growth rate. Random fracture realization is carried out in a way not to exceed the fracture density values calculated. As a first step in the global optimization technique the target is defined based on the field data available as the goal in the fracture generation. Then the difference between the random generated fracture network and the target is calculated in a weighted residual manner as:

$$E = \sum_{i=1}^{n} w_i \left(\frac{x_i - x_i^t}{x_i^t} \right)^2 \qquad (23)$$

Where i denotes the number of the fracture, w_i is the weight factor, x is the value of the fracture property and the superscript t shows the target object. The global optimization algorithm improves fracture realization in an iterative scheme to minimize this function. During the optimization process, each fracture undergoes different modifications such as shift, rotate, shrink or grow while it satisfies the predefined fracture density in the reservoir which was obtained in the tectonic simulation part. If the fracture density is exceeded, the fracture is forced to shrink or disappear. On the other hand if the fracture density obtained by the generated fracture network is lower than target fracture density map, fractures in the corresponding locations are enforced to enlarge or new fractures are inserted into the system. Also each realization is accepted with a probability which means that all the fracture realizations are used to improve the generated fracture network. The probabilities of acceptance are defined based on the objective function value between 0 and 1. The improvements continue until the objective function reaches a user-defined value or there is not any significant improvement in the objective function. Different parameters can be used in the objective functions. Also data analyses results such as statistical analysis can be used as an input to the objective function. The weighting factors are defined based on the importance of the variable. The algorithm that has been used to modify and improve the generated fracture network based on the conditional global optimization is shown in Figure 1. Also conditional aspect of the algorithm helps to fix any arbitrary properties of the fracture network as it is obtained from the field data.

Case Study

The hybrid model developed as part of this study is used to characterize Palm Valley gas reservoir in Australia. Palm Valley gas reservoir is located in the Amadeus basin in the Northern Territory. It is a nearly symmetrical East-West trending anticline. The area considered in this study trends 10,000 m in x direction, 3000 m in y direction with an average thickness of 1000 m. Field data, such as core descriptions, well logs and borehole images are collected from five wells. The folded layer is extended and compressed (reverse and forward model respectively) to reconstruct the original geological structure. The finite element mesh contains 960 elements in the horizontal plane and 15 elements in the vertical direction thus summing up to 14400 total elements. According to the Eq. (5) the thickness of the matrix layer is 650 m both above and below the reservoir layer. Also gravity force is included in the present study. The specific gravity of 2.45 for the reservoir (sandstone) and 2.75 for the layers (shale) above and below the reservoir are used. Also the initial viscosity of the reservoir layer is 6.75×10^{18} (Pa.s) which represents the estimated viscosity for sandstone (Griggs, 1939). A viscosity ratio of $\frac{\mu_1}{\mu_2} = 100$ (where, μ_1 *and* μ_2 are the viscosities of the reservoir and surrounding layer respectively) is used to cover the range of viscosities in natural folds in Palm Valley reservoir. This viscosity ratio is used as an initial guess and updated in a non-linear scheme as described previously. Boundary velocity is applied in such a way that the model's wavelength changes with a strain rate of 0.02 percent per thousand years (6.34×10^{-13} sec^{-1}) so that it is compatible with strain rate calculated by Moore and Karig (Moore and Karig, 1976). After the tectonic events are simulated in an unfolding and folding scheme, the fracture density map is generated. As part of statistical analysis bi- and uni-modal wrapped normal distribution properties for fracture azimuth and dip are identified and presented in Figure 2 and Figure 3. In the next step an initial guess is generated as the fracture network for the reservoir in a random scheme based on the fracture density map of the reservoir. Based on the wellbore values and tectonic simulation, a continuous three dimensional pixel based map of fracture density is generated. A continuous profile of fracture density along the wellbore axis for wells #1 to #4 is presented in Figure 4 and the 3D pixel based map for the reservoir in Figure 5. Conditional global optimization minimizes the scale error; however, the accuracy depends on the amount of data sources which are available from the field. Although there are different wellbore scale data available, filed scale data are limited to a few sources. This problem is reduced to a large extent by including the stress tensor map produced by the tectonic simulation. The output of the global optimization is the discrete fracture network with specific properties of each fracture such as radius, dip, and azimuth. Generated discrete fracture network is shown in Figure 6.

Conclusions

The model developed in this work presents the discrete fracture network simulation using a combination of tectonic modeling and conditional global optimization. Although global optimization minimizes the scale error, the accuracy depends on the amount of data sources available from the field which are often scarce. This problem was overcome by integrating 3D spatial map of the stress tensor for all parts of the reservoir and then fractures density which was generated by reconstructing a complex 3D folded reservoir during unfolding and folding events. This hybrid approach has allowed us to develop a comprehensive discrete fracture network map for the palm valley gas reservoir.

Selected References

Bahar, A., H. Ates, M. Al-Deeb, S. El-Abd, H. Badaam, and M. Kelkar, 2003, Practical Approach in Modeling of Naturally Fractured Reservoir : A Field Case Study: SPE 84078, 10 p. Web accessed 1 December 2011, http://www.onepetro.org/mslib/servlet/onepetropreview?id=00084078&soc=SPE

Bathe, K.-J., 1996, Finite Element Procedures. Prentice Hall, Englewood Cliffs, New Jersey, USA, 1037 p.

Biot, M.A., 1961, Theory of Folding of Stratified Viscoelastic Media and Its Implications in Tectonics and Orogenesis: GSA Bulletin 72/11, p. 1595-1620.

Bogatkov, D., and T. Babadagli, 2008, Integrated Modeling and Statistical Analysis of 3-D Fracture Network of the Midale Field: IPTC 12165, International Petroleum Technology Conference, Kuala Lumpur, Malaysia.

Cuvelier, C., A. Segal, and A. van Steenhoven, 1986, Finite Element Methods and Navier–Stokes Equations: Reidel, Dordrecht, The Netherlands, 483 p.

Cosgrove, J.W., 1999, Forced folds and fractures: An introduction *in* J.W. Cosgrove and M.S. Ameen, (eds.) Forced Foldings and Fractures: Geological Society of London, Special Publications, v. 169/1, p. 1-6.

Fisher, N.I., 1993, Statistical Analysis of Circular Data: Cambridge University Press, New York, USA, 277 p.

Fletcher, R.C., 1991, Three-dimensional folding of an embedded viscous layer in pure shear: Journal of Structural Geology, v. 13/1, p. 87-96.

Fortin, M., 1981, Old and new finite elements for incompressible flows: International Journal for Numerical Methods in Fluids, v. 1, p. 347-364.

Griffith, A.A., 1921, The Phenomena of Rupture and Flow in Solids: Philosophical Transactions of the Royal Society of London, Series A, v. 221, p. 163-198.

Griggs, D.T., 1939, Creep of Rocks, Journal of Geology, v. 47/3, p. 225-251.

Gringarten, E., 1998, FRACNET: Stochastic simulation of fractures in layered systems: Computers & Geosciences, v. 24/8, p. 729-736.

Haupt, P., 2002, Continuum Mechanics and Theory of Materials: Springer-Verlag, New York, USA, 643 p.

Hughes, T., 1987, The Finite Element Method: Prentice-Hall, Englewood Cliffs, New Jersey, USA, 631 p.

Jensen, C.L., S.H. Lee, W.J. Milliken, J. Kamath, W. Narr, H. Wu, and J.P. Davies, 1998, Field Simulation of Naturally Fractured Reservoirs Using Effective Permeabilities Derived From Realistic Fracture Characterisation: SPE 48999, 14 p. Web accessed 1 December 2011, http://www.onepetro.org/mslib/servlet/onepetropreview?id=00048999&soc=SPE

Jensen, J.L., L.W. Lake, P.W.M. Corbett, and D.J. Goggin, 2010, Statistics for Petroleum Engineers and Geoscientists, 2nd Edition: Elsevier, Amsterdam, The Netherlands, 338 p.

Johnson, A.M., 1970, Physical Processes in Geology: Freeman-Cooper, San Francisco, California, USA, 577 p.

Kaus, B.J.P., and Y.Y. Podladchikov, 2001, Forward and reverse modeling of the three dimensional viscous Rayleigh-Taylor instability: Geophysical Research Letters, v. 28/6, p. 1095-1098.

Kocher, T., and N.S. Mancktelow, 2005, Dynamic reverse modelling of flanking structures: a source of quantitative kinematic information: Journal of Structural Geology v. 27/8, p. 1346-1354.

Moore, J.C., and D.E. Karig, 1976, Sedimentology, structural geology, and tectonics of the Shikoku subduction zone, southwestern Japan: GSA Bulletin, v. 87/9, p. 1259-1268.

Nelson, R.A., 1985, Geologic Analysis of Naturally Fractured Reservoirs: Gulf Publishing Company, Houston, Texas, USA, 335 p.

O'Driscoll, E.S., 1962, Experimental patterns in superimposed similar folding: Alberta Society of Petroleum Geology Journal, v. 10/3, p. 145-167.

P. Jager, S.M. Schmalholz, D.W. Schmid, and E. Kuhl, 2008, Brittle fracture during folding of rocks: A finite element study: Philosophical Magazine, v. 88/28-29, p. 3245-3263.

Pastor, M., M. Quecedo, and O.C. Zienkiewicz, 1997, A mixed displacement-pressure formulation for numerical analysis of plastic failure: Computers & Structures, v. 62/1, p. 13-23.

Price, N.J., 1966, Fault and joint development in brittle and semi-brittle rock: Pergamon Press, Oxford, England, 176 p.

Rafiee, A., and M. Vinches, 2008, Application of Geostatistical Characteristics of Rock Mass Fracture Systems in 3D Model Generation: International Journal of Rock Mechanics and Mining Sciences, v. 45, p. 664-652.

Ramberg, H., 1963, Fluid dynamics of viscous buckling applicable to folding of layered rocks: AAPG Bulletin, v. 47/3, p. 484-505.

Ramsay, J.G., and M.I. Huber, 1983, The Techniques of Modern Structural Geology, Volume 1: Strain Analysis: Academic Press, London, England, 307 p.

Reddy, J.N., R.J. Stein, and J.S. Wickham, 1983, Finite-element modeling of folding and faulting: International Journal for Numerical and Analytical Methods in Geomechanics, v. 6, p. 425-440.

Sahimi, M., 1995, New Models for Natural and Hydraulic Fracturing of Heterogeneous Rock: SPE 29648, 16 p. Web accessed 1 December 2011, http://www.onepetro.org/mslib/servlet/onepetropreview?id=00029648&soc=SPE

Schmalholz, S.M., 2008, 3D numerical modeling of forward folding and reverse unfolding of a viscous single-layer: Implications for the formation of folds and fold patterns: Tectonophysics, v. 446/1-4, p. 31-41.

Tamagawa, T.M., T. Matsuura, T. Anraku, K. Tezuka, and T. Namikawa, 2002, Construction of Fracture Network Model Using Static and Dynamic Data: SPE 77741, 12 p. Web accessed 1 December 2011, http://www.onepetro.org/mslib/servlet/onepetropreview?id=00077741&soc=SPE

Tran, N.H., C.Zhixi, and S.S. Rahman, 2006, Integrated conditional global optimization for discrete fracture network modeling: Computers and Geosciences, v. 32/1, p. 17-27.

Wickham, J.S., G.S. Tapp, and J.N. Reddy, 1982, Finite-element modeling of fracture density in single layer folds: International Journal for Numerical and Analytical Methods in Geomechanics, v. 6/4, p. 441-459.

Zienkiewicz, O.C., and R.L. Taylor, 2000, The Finite Element Method for Fluid Dynamics, Fifth Edition, Volume 3: Butterworth-Heinemann, Woburn, Massachusetts, USA, 334 p.

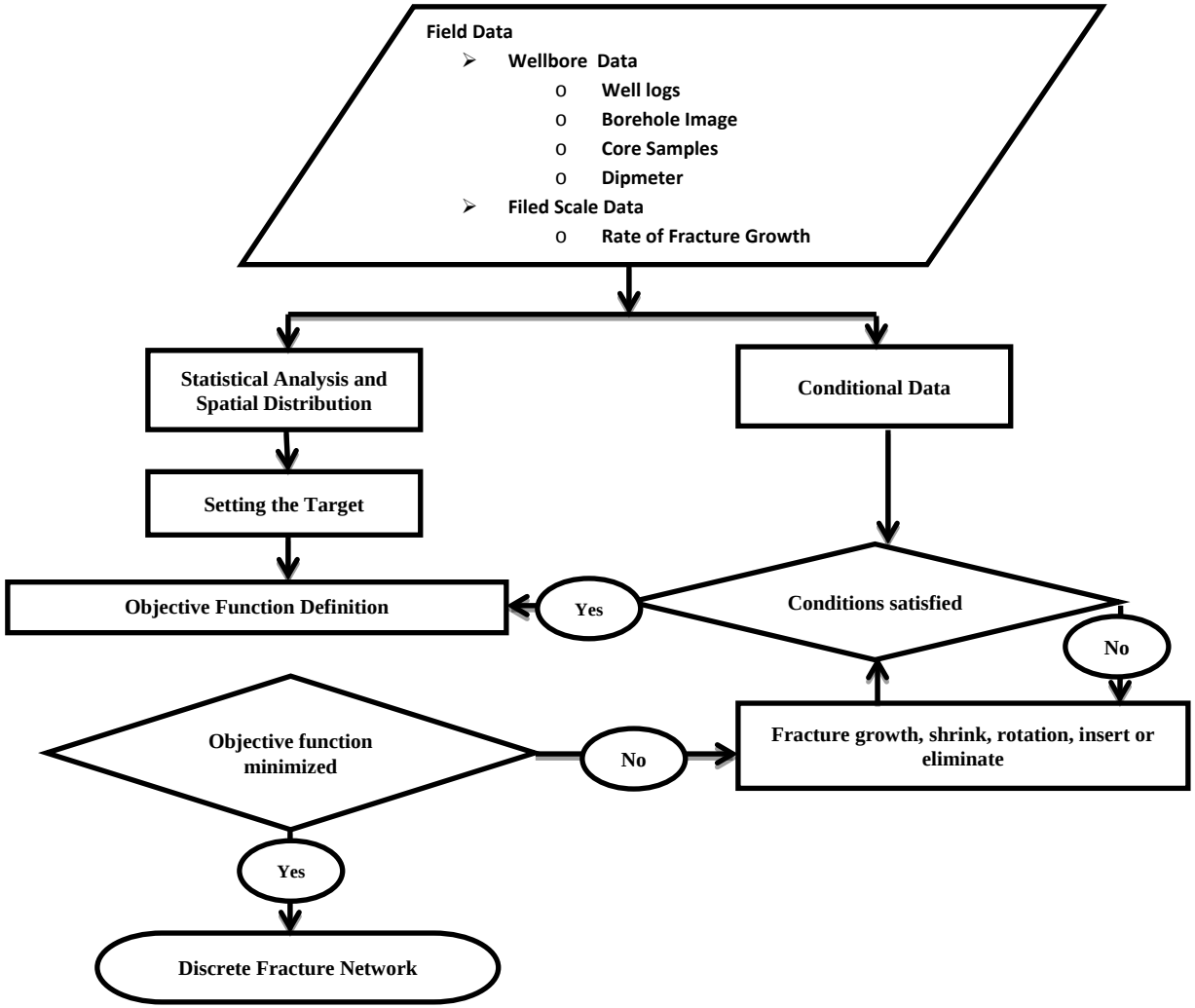

Figure 1. Algorithm for conditional global optimization process to generate the fracture network.

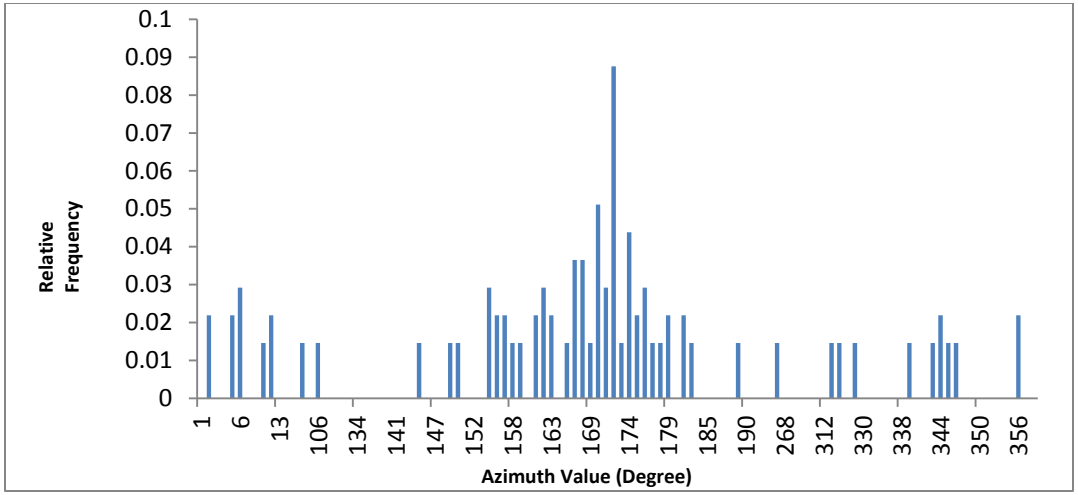

Figure 2. Circular statistical analysis: histogram and probability density function plot for fracture azimuth. Statistical analysis on the circular azimuth data reveals a bimodal wrapped normal distribution, with modes at approximately 6° and 172°.

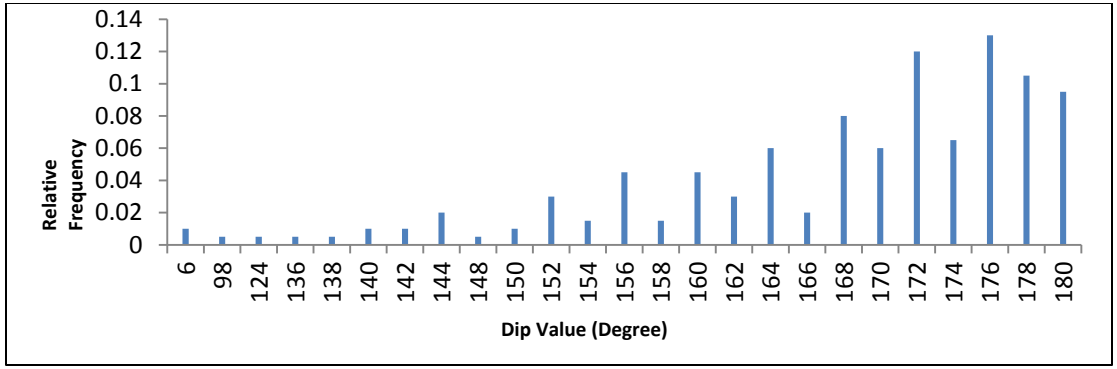

Figure 3. Circular statistical analysis: histogram and probability density function plot for fracture dip showing one-modal wrapped normal distribution, whose mode is at 176°.

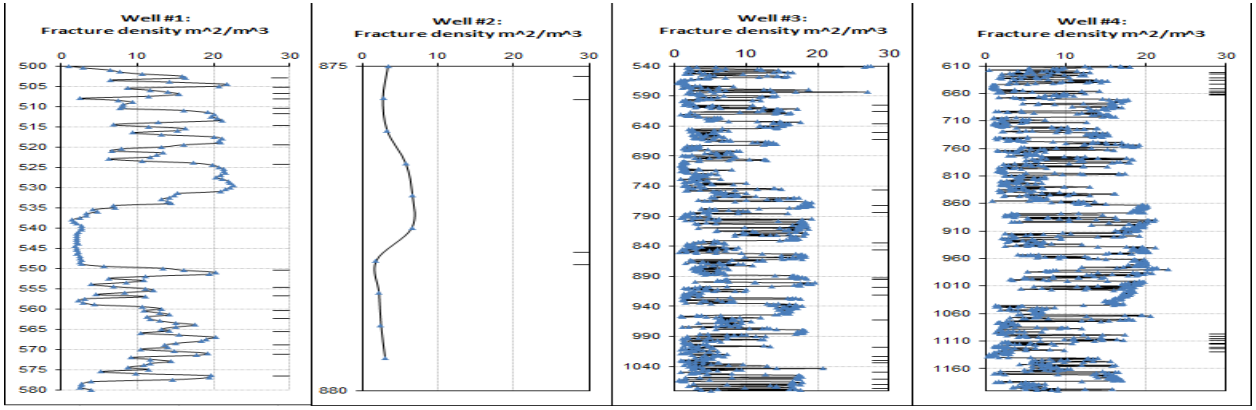

Figure 4. Fracture density values in four sells. The locations of available hard data are shown by solid dashed lines in the right side of the graphs.

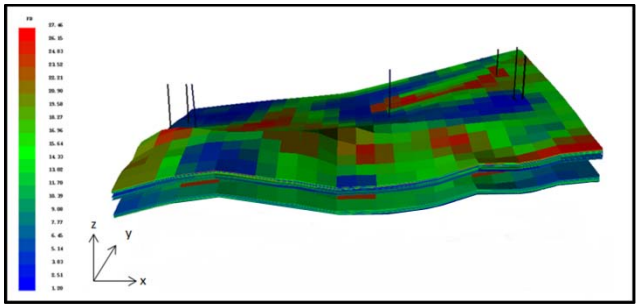

Figure 5. 3D pixel based map of the fracture density for all parts of the reservoir.

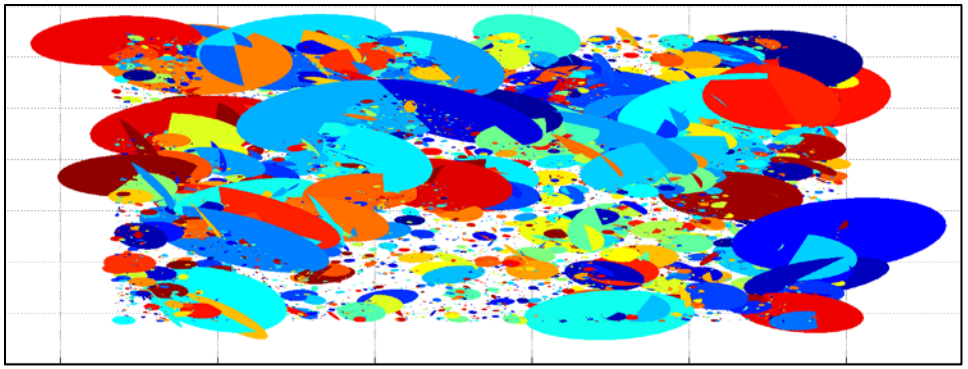

Figure 6. Discrete fracture network of palm valley gas reservoir (P1 unit of horizon).